

Article

## Eurothiocin A and B, Sulfur-Containing Benzofurans from a Soft Coral-Derived Fungus *Eurotium rubrum* SH-823

Zhaoming Liu, Guoping Xia, Senhua Chen, Yayue Liu, Hanxiang Li \* and Zhigang She \*

School of Chemistry and Chemical Engineering, Sun Yat-Sen University, Guangzhou 510275, China; E-Mails: liuzhaom@mail2.sysu.edu.cn (Z.L.); xiagp@mail2.sysu.edu.cn (G.X.); chensh65@mail2.sysu.edu.cn (S.C.); liuyayue@mail2.sysu.edu.cn (Y.L.)

\* Authors to whom correspondence should be addressed; E-Mails: lihx3@mail.sysu.edu.cn (H.L.); ceshzhg@mail.sysu.edu.cn (Z.S.); Tel./Fax: +86-20-8411-3356.

Received: 30 April 2014; in revised form: 3 June 2014 / Accepted: 13 June 2014 /

Published: 20 June 2014

---

**Abstract:** Two new sulfur-containing benzofuran derivatives, eurothiocin A and B (**1** and **2**), along with five known compounds, zinniol (**3**), butyrolactone I (**4**), aspernolide D (**5**), vermistatin (**6**), and methoxyvermistatin (**7**), were isolated from the cultures of *Eurotium rubrum* SH-823, a fungus obtained from a *Sarcophyton* sp. soft coral collected from the South China Sea. The new compounds (**1** and **2**) share a methyl thiolester moiety, which is quite rare among natural secondary metabolites. The structures of these metabolites were assigned on the basis of detailed spectroscopic analysis. The absolute configurations of **1** and **2** were determined by comparison of the experimental and calculated electronic circular dichroism (ECD) data. Compounds **1** and **2** exhibited more potent inhibitory effects against  $\alpha$ -glucosidase activity than the clinical  $\alpha$ -glucosidase inhibitor acarbose. Further mechanistic analysis showed that both of them exhibited competitive inhibition characteristics.

**Keywords:** marine fungi; secondary metabolites;  $\alpha$ -glucosidase inhibitor; theoretical calculations; ECD; TDDFT

---

### 1. Introduction

In the search for new pharmaceutical lead compounds, increasing attention is being given to marine fungi [1–3]. As marine fungi survive under harsh environmental conditions, it can be expected that they may have evolved to biosynthesize biologically interesting and chemically diverse compounds [3].



## 2. Results and Discussion

Eurothiocin A (**1**) was obtained as a colorless oil. ESIMS data exhibited apparent molecular ions at 281.2  $[M + H]^+$  and 283.2  $[M + H + 2]^+$  in a 20:1 ratio, consistent with a compound containing a sulfur atom [30]. The molecular formula was subsequently determined as  $C_{14}H_{18}O_4S$  on the basis of HREIMS ( $m/z$  282.1621  $[M]^+$ , calcd 282.1618), indicating six degrees of unsaturation. The UV spectrum of **1** showed absorption maxima at 239 (sh) and 302 nm. The  $^1H$  spectrum in  $CDCl_3$  (Table 1) exhibited the presence of four singlet methyls (Me-2', Me-3', Me-5', and Me-6'), one methylene ( $H_2-3$ ), one oxymethine (H-2), one aromatic proton (H-7), and one chelated phenolic hydroxyl group (4-OH). These findings were in agreement with the  $^{13}C$  NMR and DEPT data (Table 1), which exhibited 14 carbon signals as a carbonyl group ( $\delta_C$  197.7), two oxygenated  $sp^3$ -hybridized carbons ( $\delta_C$  91.3 and  $\delta_C$  71.9), one methylene ( $\delta_C$  27.7), four methyls ( $\delta_C$  25.8, 23.8, 25.0, and 13.0), in addition to six  $sp^2$ -hybridized carbons that were assigned to a pentasubstituted benzene ring. These functionalities, *i.e.*, one benzene ring and one carbonyl, account for five degrees of unsaturation, thus indicating one more ring being present in the molecule to satisfy the one remaining degree of unsaturation.

**Table 1.** NMR spectroscopic data ( $CDCl_3$ , 400/100 MHz) for **1** and **2**<sup>a</sup>.

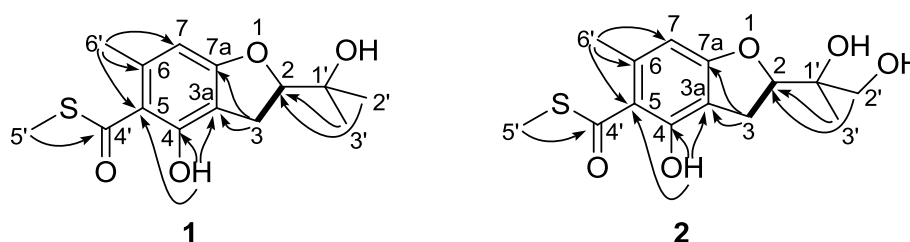
Position	<b>1</b>		<b>2</b>	
	$\delta_C$	$\delta_H$	$\delta_C$	$\delta_H$
2	91.3, C	4.71, dd (9.5, 8.4)	87.2, C	4.90, t (8.8)
3	27.7, CH <sub>2</sub>	3.05, dd (15.6, 8.4) 3.14, dd (15.6, 9.5)	27.2, CH <sub>2</sub>	3.17, d (8.8)
3a	111.5, C	-	111.3, C	-
4	158.2, C	-	158.2, C	-
5	116.1, C	-	116.2, C	-
6	141.8, C	-	141.9, C	-
7	105.7, CH	6.26, s	105.7, CH	6.24, s
7a	164.3, C	-	164.1, C	-
1'	71.9, C	-	73.7, C	-
2'	25.8, CH <sub>3</sub>	1.33, s	66.9, CH <sub>2</sub>	3.53, d (11.0) 3.75, d (11.0)
3'	23.8, CH <sub>3</sub>	1.22, s	19.1, CH <sub>3</sub>	1.20, s
4'	197.7, C	-	197.8, C	-
5'	13.0, CH <sub>3</sub>	2.47, s	13.1, CH <sub>3</sub>	2.46, s
6'	25.0, CH <sub>3</sub>	2.69, s	25.1, CH <sub>3</sub>	2.68, s
4-OH	-	11.83, brs	-	11.83, brs

<sup>a</sup>  $\delta$  in ppm,  $J$  in Hz, TMS as internal standard.

Extensive analysis by 2D NMR, including HSQC, HMBC, and COSY, revealed the planar structure of eurothiocin A (**1**) as described below (Figure 1). In the  $^1H-^1H$  COSY spectrum, the oxymethine proton H-2 was correlated to the methylene protons  $H_2-3$ , revealing the connectivity of C-2 to C-3. HMBC cross-peaks from  $H_2-3$  to C-3a, C-7a, and C-4 and from H-2 to C-3a and C-7a established the dihydrobenzofuran ring with connectivity of C-2 to C-7a via an oxygen atom. Further correlations from *gem*-dimethyl groups ( $H_3-2'$  and  $H_3-3'$ ) to C-1' and C-2 indicated that the oxygenated  $sp^3$

quaternary carbon C-1' was attached to C-2', C-3', and C-2. The aromatic methyl signal H<sub>3</sub>-6' ( $\delta_{\text{H}}$  2.69) exhibited HMBC correlations to C-5, C-6, and C-7, establishing the location of this methyl group. An additional four-bond W-type correlation from H<sub>3</sub>-6' to the carbonyl carbon C-4' connected C-4' to C-5. The phenolic hydroxyl 4-OH was placed *ortho* to the carbonyl substituent C-4' on the basis of its <sup>1</sup>H NMR chemical shift ( $\delta_{\text{H}}$  11.83), as well as the HMBC correlations of its proton to C-3a, C-4, and C-5. Lastly, the presence of a methyl thioester was revealed by HMBC correlations of the S-CH<sub>3</sub> methyl protons ( $\delta_{\text{H}}$  2.47) to the carbonyl carbon C-4' ( $\delta_{\text{C}}$  197.7), and the <sup>1</sup>H and <sup>13</sup>C NMR chemical shifts for S-CH<sub>3</sub> ( $\delta_{\text{H}}/\delta_{\text{C}}$  2.47/13.0) which are characteristic of a methyl thiolester group [31,32]. Moreover, the base peak in the EIMS spectrum corresponds to loss of 47 mass units, which is consistent with the expected [M – SCH<sub>3</sub>]<sup>+</sup> fragmentation peak [32]. These data led to the assignment of the structure of eurothiocin A (**1**) as shown.

**Figure 1.** Selected <sup>1</sup>H–<sup>1</sup>H COSY (bold line) and HMBC (arrow) correlations of compounds **1** and **2**.



To assign the absolute configuration of **1**, ECD spectrum was measured in MeCN solution and compared with those calculated by quantum-mechanics. The conformational analyses of (*R*)-**1** were carried out with molecular mechanics (using the Merck molecular force field, MMFF) based on a Monte Carlo algorithm. Eight conformers with relative energy within 1 kcal/mol were generated and further geometry-optimized at CAM-B3LYP/aug-cc-pVDZ level using Gaussian 03 program. Four stable conformers were obtained (Figure 2), and frequency analyses were performed at the same level to show no imaginary frequencies. ECD spectra for the four conformers were calculated using TD-DFT method at CAM-B3LYP/aug-cc-pVDZ level. The final Boltzmann factor-weighted theoretical ECD spectrum (Figure 3 and Supplementary Figure S15) was similar to the experimental ECD spectrum, which showed a positive Cotton effect at 241 nm and a strong negative Cotton effect at 302 nm, respectively. Thus, the absolute configuration of compound **1** was established as *R*.

Eurothiocin B (**2**) was isolated as a white amorphous solid. Its HREIMS spectrum displayed a molecular ion peak at  $m/z$  [M]<sup>+</sup> 298.0942 (calcd 298.0941), corresponding to the molecular formula C<sub>14</sub>H<sub>18</sub>O<sub>5</sub>S. The <sup>1</sup>H and <sup>13</sup>C NMR spectra together with HSQC correlations for eurothiocin B (**2**) showed one carbonyl carbon (C-4',  $\delta_{\text{C}}$  197.8), six sp<sup>2</sup>-hybridized quaternary (one protonated), two methylenes (C-3 and C-2', one of which was oxygenated), one oxymethine (C-2), one oxygenated quaternary carbon (C-1'), and three methyls (Me-3', Me-5', and Me-6'). A detailed comparison of the NMR data with those for eurothiocin A (**1**) revealed that **2** differed from **1** only at C-2'. The methyl signal at  $\delta_{\text{H}}$  1.33 (s, H-2') and  $\delta_{\text{C}}$  25.8 (C-2') observed in the spectrum of **1** were replaced by oxygenated methylene protons at  $\delta_{\text{H}}$  3.53 and 3.75 (both d,  $J$  = 11.0 Hz) and  $\delta_{\text{C}}$  66.9 (C-2') in the NMR spectrum of **2**, which suggested that **2** is a 2'-oxygenated derivative of **1**. HMBC correlations from

H<sub>3</sub>-3' to C-1', C-2', and C-2, from H<sub>2</sub>-2' to C-1', C-3', and C-2, and from H-2 to C-1', C-2' and C-3', further supported the proposed planar structure for **2**.

**Figure 2.** Most stable conformers of (*R*)-**1** calculated at the DFT/CAM-B3LYP/aug-cc-pVDZ level of theory. Relative populations are in parentheses.

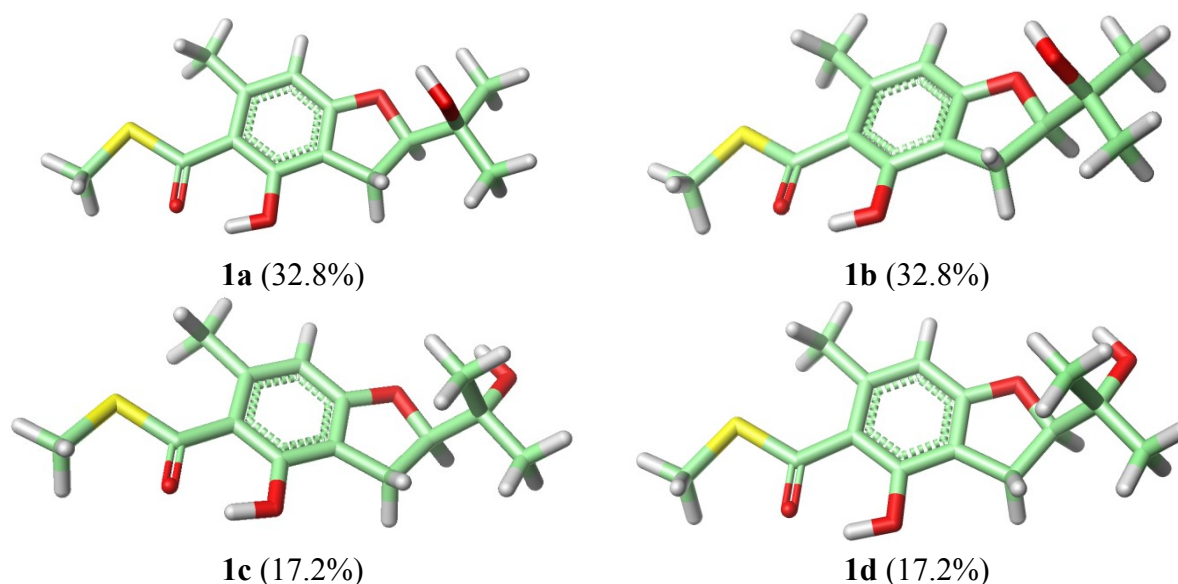
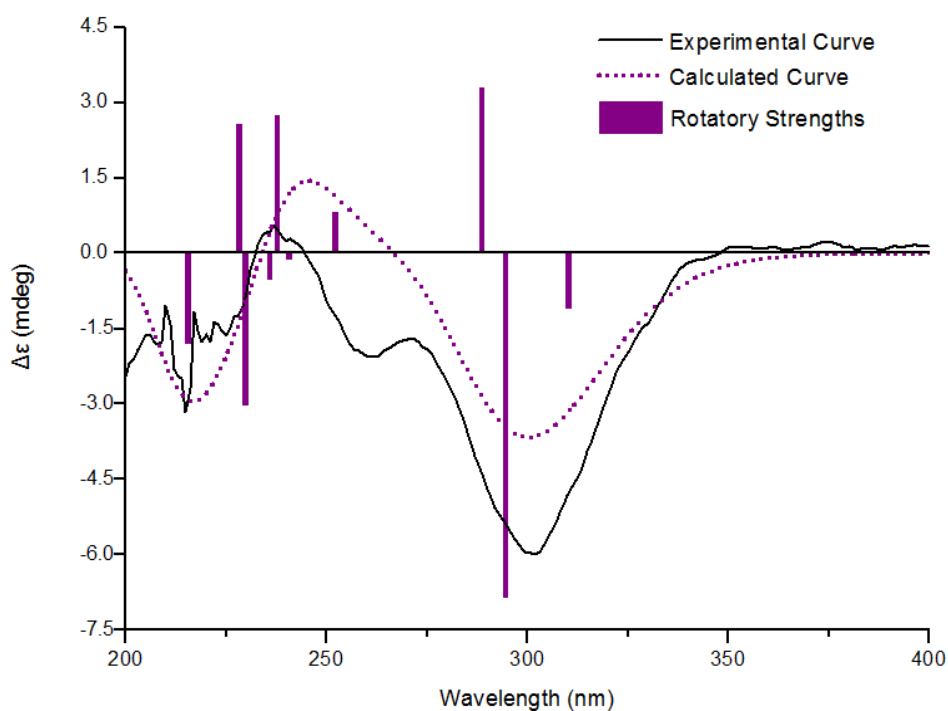


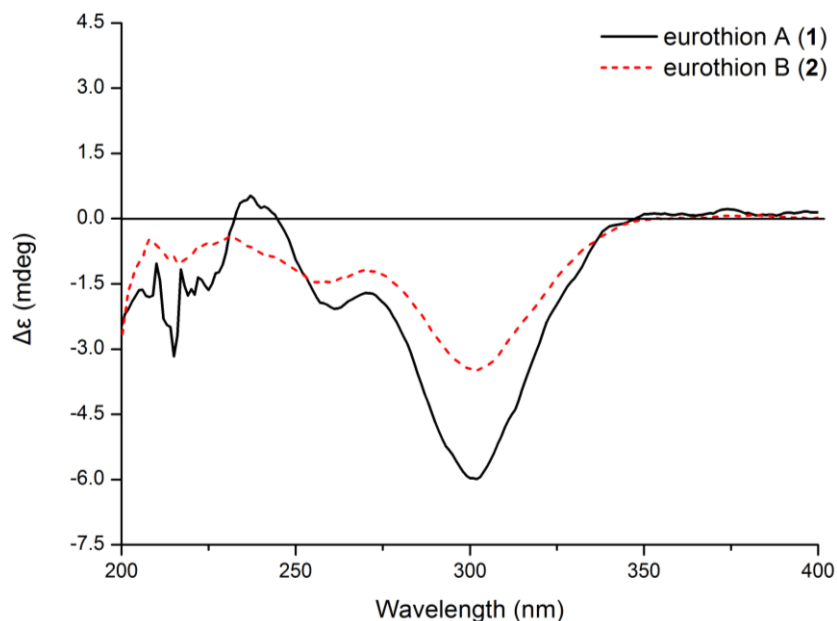
**Figure 3.** Experimental and calculated electronic circular dichroism (ECD) spectra of **1**<sup>a</sup>.



<sup>a</sup> Black solid line: ECD spectrum of **1** in MeCN solution. Purple dotted line: calculated ECD spectrum for (*R*)-**1** with CAM-B3LYP/aug-cc-pVDZ method on DFT-optimized structure. Purple bars: rotational strength values of the lowest-energy conformer of (*R*)-**1** optimized with CAM-B3LYP/aug-cc-pVDZ.

According to comparison of the CD spectrum with that of **1** and their structural similarities (Figure 4), the absolute configuration at C-2 of eurothiocin B (**2**) is proposed to be the same as in eurothiocin A (**1**), but the stereochemistry at C-1' of the side chain is unknown. Consequently, the overall absolute configuration of eurothiocin B (**2**) remains to be determined.

**Figure 4.** Comparison of experimental ECD spectra of eurothion A (**1**) and B (**2**).



The structures of the known compounds were identified as zinniol (**3**) [33], butyrolactone I (**4**) [34], aspernolide D (**5**) [35], vermistatin (**6**) [36,37], and methoxyvermistatin (**7**) [37], by comparison of their spectroscopic data and optical rotations with those reported in the literature.

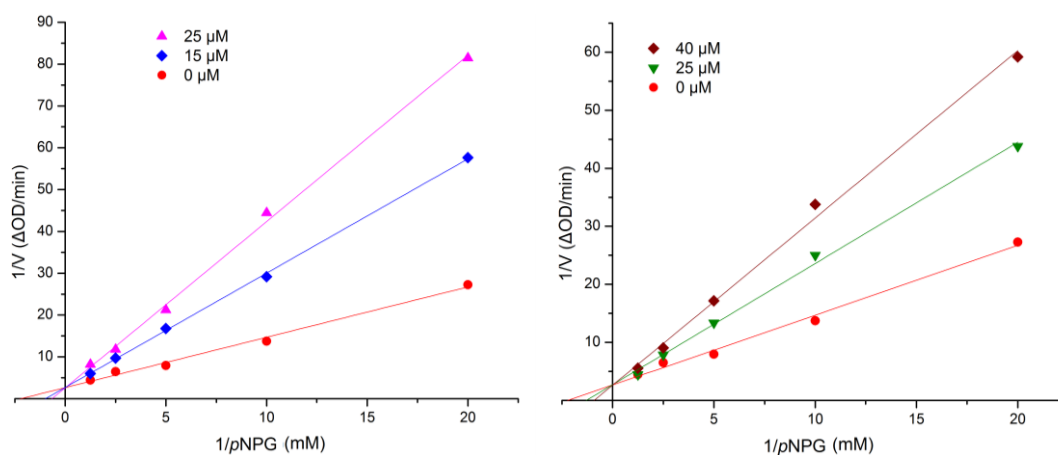
The  $\alpha$ -glucosidase inhibitory effects of the isolates were evaluated along with the clinical  $\alpha$ -glucosidase inhibitor acarbose (positive control). As a result (Table 2), the compounds **1** and **2** were the most active, and showed better inhibitory potential ( $IC_{50} = 17.1$  and  $42.6 \mu\text{M}$ , respectively) than acarbose ( $IC_{50} = 376.7 \mu\text{M}$ ). In order to examine the type of inhibition of the new compounds **1** and **2**, further kinetic studies were carried out by the Lineweaver-Burk plot method. The results are shown in Figure 5, indicating that **1** and **2** are competitive inhibitors of  $\alpha$ -glucosidase. More details are in the Supplementary Information.

**Table 2.**  $\alpha$ -Glucosidase Inhibitory Activities <sup>a</sup>.

Compounds	<b>1</b>	<b>2</b>	<b>4</b>	<b>5</b>	<b>6</b>	<b>7</b>	Acarbose <sup>b</sup>
$IC_{50}$ ( $\mu\text{M}$ )	$17.1 \pm 0.7$	$42.6 \pm 1.4$	$98.5 \pm 3.3$	$110.8 \pm 1.7$	$107.1 \pm 2.6$	$236 \pm 4.2$	$376.7 \pm 5.2$

<sup>a</sup>  $IC_{50}$  values are shown as mean  $\pm$  SD from two independent experiments. The inhibitory activity of compound **3** was not tested due to the limited amount; <sup>b</sup> Positive control.

**Figure 5.** Kinetic analysis of the inhibition of  $\alpha$ -glucosidase by compounds **1** (left) and **2** (right). More details are in the Supplementary Information.



### 3. Experimental Section

#### 3.1. General

Melting points were measured on an X-4 micromeltin-point apparatus (Cany Precision Instruments Co., Ltd., Shanghai, China) and are uncorrected. Optical rotations were recorded with an MCP 300 (Anton Paar, Shanghai, China) polarimeter at 25 °C. UV data were measured on a UV-240 spectrophotometer (Shimadzu, Beijing, China). CD data were recorded with a J-810 spectropolarimeter (JASCO, Tokyo, Japan). The NMR data were recorded on a Bruker Avance 400 spectrometer (Bruker, Beijing, China) at 400 MHz for  $^1\text{H}$  and 100 MHz for  $^{13}\text{C}$  in  $\text{CDCl}_3$ , respectively. All chemical shifts ( $\delta$ ) are given in ppm with reference to TMS, and coupling constants (J) are given in Hz. LRESIMS spectra were recorded on a Finnigan LCQ-DECA mass spectrometer (Finnigan, Beijing, China). EIMS on a DSQ EI-mass spectrometer (Thermo, Shanghai, China) and HREIMS data were measured on a MAT95XP high-resolution mass spectrometer (Thermo). Column chromatography (CC) was performed on silica gel (200–300 mesh, Qingdao Marine Chemical Factory, Qingdao, China) and Sephadex LH-20 (Amersham Pharmacia, Piscataway, NJ, USA). Precoated silica gel plates (Qingdao Huang Hai Chemical Group Co., Qingdao, China; G60, F-254) were used for thin layer chromatography. Semipreparative HPLC was performed on a Waters Breeze HPLC system using a Phenomenex Luna (Phenomenex, Torrance, CA, USA)  $\text{C}_{18}$  column (250  $\times$  10 mm, 5  $\mu\text{m}$ ), flow rate, 2.0 mL/min.

#### 3.2. Fungal Material

The fungal strain used in this study was isolated from a piece of fresh tissue from the inner part of the soft coral *Sarcophyton* sp., which was collected from Xuwen National Coral Reef Nature Reserve in the South China Sea in September 2012. It was obtained using the standard protocol for the isolation of endophytic microbes. This isolate was identified by Hanxiang Li and assigned the accession number SH-823. A voucher strain was deposited in School of Chemistry and Chemical Engineering, Sun Yat-sen University, Guangzhou, China.

### 3.3. Extraction and Isolation

The fungus *E. rubrum* SH-823 was fermented on autoclaved rice solid-substrate medium (twenty 500 mL Erlenmeyer flasks, each containing 50 g of rice and 50 mL of distilled water) for 30 days at 25 °C. Following incubation, the mycelia and solid rice medium were extracted with EtOAc. The organic solvent was filtered and concentrated under reduced pressure to yield 4.7 g of organic extract. The extract was subjected to silica gel CC using gradient elution with petroleum ether-EtOAc from 90:10 to 0:100 (v/v) to give twelve fractions (Frs.1–12). Fr. 4 (517 mg) was further purified by silica gel CC using 30% EtOAc-light petroleum to afford seven subfractions (Frs.4.1–4.7). Fr.4.3 (35 mg) was applied to Sephadex LH-20 CC, eluted with CHCl<sub>3</sub>/MeOH (1:1), to obtain eight subfractions (Frs.4.3.1–F4.3.8). Fr.4.3.4 (14 mg) was further purified by RP-HPLC (70% MeOH in H<sub>2</sub>O for 5 min, followed by 70%–100% over 25 min; 2.0 mL/min) to afford **1** (2.7 mg, *t<sub>R</sub>* 16.5 min) and **2** (1.6 mg, *t<sub>R</sub>* 23.0 min).

**Compound 1:** Colorless oil;  $[\alpha]_D^{25}$   $-135$  (*c* 0.20, MeCN); UV (MeOH) ( $\lambda_{\max}$ ) (log  $\epsilon$ ) 239 (sh), 302 (3.97) nm; <sup>1</sup>H and <sup>13</sup>C NMR spectroscopic data, see Table 1; EIMS *m/z* 282 [M]<sup>+</sup>, HREIMS *m/z* 282.1621 ([M]<sup>+</sup>, C<sub>14</sub>H<sub>18</sub>O<sub>4</sub>S, calcd 282.1618).

**Compound 2:** White amorphous power (CHCl<sub>3</sub>); m.p. 122–123 °C;  $[\alpha]_D^{25}$   $-69$  (*c* 0.29, MeCN); UV (MeOH) ( $\lambda_{\max}$ ) (log  $\epsilon$ ) 243 (sh), 301 (3.95) nm; <sup>1</sup>H and <sup>13</sup>C NMR spectroscopic data, see Table 1; EIMS *m/z* 298 [M]<sup>+</sup>, HREIMS *m/z* 298.0942 [M]<sup>+</sup> (C<sub>14</sub>H<sub>18</sub>O<sub>5</sub>S, calcd 298.0941).

### 3.4. Calculation of ECD Spectra

Molecular mechanics calculations were run with Spartan '10 (Wavefunction, Inc., Irvine, CA, USA) with standard parameters and convergence criteria. DFT and TDDFT calculations were run with Gaussian 03 (Gaussian, Wallingford, CT, USA) with default grids and convergence criteria. TDDFT calculations were carried out by using CAM-B3LYP/aug-cc-pVDZ method and included 10 single excited states in each case. The IEF-PCM solvent model for MeCN was included in all cases. ECD spectra were generated using the program SpecDis 1.6 (University of Würzburg, Würzburg, Germany) and OriginPro 8.5 (OriginLab, Ltd., Northampton, MA, USA) from dipole-length rotational strengths by applying Gaussian band shapes with sigma = 0.40 eV and UV shift = +24 nm. All calculations were performed with High-Performance Grid Computing Platform of Sun Yat-Sen University.

### 3.5. Assay for $\alpha$ -Glucosidase Inhibitory Activity

$\alpha$ -Glucosidase was assayed according to standard procedures [38,39] by following the hydrolysis of nitrophenyl glycosides by monitoring formation of *p*-nitrophenol spectrometrically at 400 nm. The reaction mixture (final volume, 1 mL) consisted of the enzyme solution (20  $\mu$ L, Sigma 9001-42-7, E.C 3.2.1.20), substrate (10 mM *p*-nitrophenyl- $\alpha$ -glucopyranoside, 20  $\mu$ L, Fluka, BioChemika, Buchs, Switzerland) in 50 mM potassium phosphate buffer (pH 7.0) and test sample dissolved in DMSO (20  $\mu$ L). The inhibitors were pre-incubated with the enzyme at 37 °C for 30 min, and the substrate was then added. The reaction was monitored spectrophotometrically by measuring the absorbance at 400 nm. Acarbose was used as a positive control. The inhibitory activity of test compound was determined

as a percentage in comparison to a blank according with the following equation: The inhibition rates (%) =  $[(OD_{\text{control}} - OD_{\text{control blank}}) - (OD_{\text{test}} - OD_{\text{test blank}})] / (OD_{\text{control}} - OD_{\text{control blank}}) \times 100\%$ . The IC<sub>50</sub> values of compounds were calculated by the nonlinear regression analysis and expressed as the mean  $\pm$  SD of two distinct experiments. Kinetic parameters were determined using the Lineweaver-Burk double-reciprocal plot method at increasing concentration of substrates and inhibitors.

#### 4. Conclusions

Chemical investigation of a soft coral-derived fungus *Eurotium rubrum* SH-823 led to the discovery of two new sulfur-containing benzofurans, eurothiocin A (**1**) and B (**2**), together with five known compounds, zinniol (**3**), butyrolactone I (**4**), aspernolide D (**5**), vermistatin (**6**), and methoxyvermistatin (**7**). To the best of our knowledge, the presence of a methyl thiolester group is quite rare among secondary metabolites. Two examples resembling compounds **1** and **2** are mortivinacin [31] and resorthiomycin [40,41], which were isolated from *Mortierella vinacea* and *Streptomyces collinus*, respectively. The isolated compounds were evaluated for their  $\alpha$ -glucosidase inhibitory effects. Compounds **1** and **2** exhibited more potent inhibitory effects against  $\alpha$ -glucosidase activity than the clinical  $\alpha$ -glucosidase inhibitor acarbose. Further mechanistic analysis showed that the two compounds exhibited competitive inhibition characteristics.

#### Acknowledgments

This research was financially supported by the National Natural Science Foundation of China (41376149, 41276146), the 863 Foundation of China (2011AA09070201), the Science & Technology Plan Project of Guangdong Province of China (2010B030600004, 2011A080403006), the Guangzhou Project of Science & Technology Planning (No. 2010J1-E331), the China Postdoctoral Science Foundation (2013M542224) and the China's Marine Commonweal Research Project (201005022-2). We also thank High-Performance Grid Computing Platform of Sun Yat-Sen University for the support of our computational chemistry research.

#### Author Contributions

Conceived and designed the experiments: Hanxiang Li, Zhigang She, Zhaoming Liu, Senhua Chen. Performed the experiments: Zhaoming Liu, Senhua Chen, Yayue Liu. Analyzed the data: Zhaoming Liu, Senhua Chen, Guoping Xia, Hanxiang Li. Wrote the paper: Zhaoming Liu, Hanxiang Li, Guoping Xia. Read and approved the final manuscript: Hanxiang Li, Zhigang She, Guoping Xia.

#### Conflicts of Interest

The authors declare no conflict of interest.

#### References

1. Blunt, J.W.; Copp, B.R.; Keyzers, R.A.; Munro, M.H.; Prinsep, M.R. Marine natural products. *Nat. Prod. Rep.* **2014**, *31*, 160–258.

2. Blunt, J.W.; Copp, B.R.; Keyzers, R.A.; Munro, M.H.; Prinsep, M.R. Marine natural products. *Nat. Prod. Rep.* **2013**, *30*, 237–323.
3. Rateb, M.E.; Ebel, R. Secondary metabolites of fungi from marine habitats. *Nat. Prod. Rep.* **2011**, *28*, 290–344.
4. König, G.M.; Kehraus, S.; Seibert, S.F.; Abdel-Lateff, A.; Müller, D. Natural products from marine organisms and their associated microbes. *ChemBioChem* **2006**, *7*, 229–238.
5. Watts, K.R.; Loveridge, S.T.; Tenney, K.; Media, J.; Valeriote, F.A.; Crews, P. Utilizing DART mass spectrometry to pinpoint halogenated metabolites from a marine invertebrate-derived fungus. *J. Org. Chem.* **2011**, *76*, 6201–6208.
6. Menezes, C.B.; Bonugli-Santos, R.C.; Miqueletto, P.B.; Passarini, M.R.; Silva, C.H.; Justo, M.R.; Leal, R.R.; Fantinatti-Garboggini, F.; Oliveira, V.M.; Berlinck, R.G.; *et al.* Microbial diversity associated with algae, ascidians and sponges from the north coast of São Paulo state, Brazil. *Microbiol. Res.* **2010**, *165*, 466–482.
7. Radjasa, O.K.; Vaske, Y.M.; Navarro, G.; Vervoort, H.C.; Tenney, K.; Linington, R.G.; Crews, P. Highlights of marine invertebrate-derived biosynthetic products: their biomedical potential and possible production by microbial associates. *Bioorg. Med. Chem.* **2011**, *19*, 6658–6674.
8. Unson, M.D.; Holland, N.D.; Faulkner, D.J. A brominated secondary metabolite synthesized by the cyanobacterial symbiont of a marine sponge and accumulation of the crystalline metabolite in the sponge tissue. *Mar. Biol.* **1994**, *119*, 1–11.
9. Unson, M.D.; Faulkner, D.J. Cyanobacterial symbiont biosynthesis of chlorinated metabolites from *Dysidea herbacea* (Porifera). *Experientia* **1993**, *49*, 349–353.
10. Wang, C.Y.; Wang, B.G.; Brauers, G.; Guan, H.S.; Proksch, P.; Ebel, R. Microsphaerones A and B, two novel  $\gamma$ -pyrone derivatives from the sponge-derived fungus *Microsphaeropsis* sp. *J. Nat. Prod.* **2002**, *65*, 772–775.
11. Thomas, T.R.; Kavlekar, D.P.; LokaBharathi, P.A. Marine drugs from sponge-microbe association—A review. *Mar. Drugs* **2010**, *8*, 1417–1468.
12. Saleem, M.; Ali, M.S.; Hussain, S.; Jabbar, A.; Ashraf, M.; Lee, Y.S. Marine natural products of fungal origin. *Nat. Prod. Rep.* **2007**, *24*, 1142–1152.
13. Suciati Fraser, J.A.; Lambert, L.K.; Pierens, G.K.; Bernhardt, P.V.; Garson, M.J. Secondary metabolites of the sponge-derived fungus *Acremonium persicinum*. *J. Nat. Prod.* **2013**, *76*, 1432–1440.
14. Amend, A.S.; Barshis, D.J.; Oliver, T.A. Coral-associated marine fungi form novel lineages and heterogeneous assemblages. *ISME J.* **2012**, *6*, 1291–1301.
15. Knowlton, N.; Rohwer, F. Multispecies microbial mutualisms on coral reefs: The host as a habitat. *Am. Nat.* **2003**, *162*, S51–S62.
16. Rosenberg, E.; Koren, O.; Reshef, L.; Efrony, R.; Zilber-Rosenberg, I. The role of microorganisms in coral health, disease and evolution. *Nat. Rev. Microbiol.* **2007**, *5*, 355–362.
17. Wegley, L.; Edwards, R.; Rodriguez-Brito, B.; Liu, H.; Rohwer, F. Metagenomic analysis of the microbial community associated with the coral *Porites astreoides*. *Environ. Microbiol.* **2007**, *9*, 2707–2719.

18. Zheng, C.J.; Shao, C.L.; Guo, Z.Y.; Chen, J.F.; Deng, D.S.; Yang, K.L.; Chen, Y.Y.; Fu, X.M.; She, Z.G.; Lin, Y.C.; Wang, C.Y. Bioactive hydroanthraquinones and anthraquinone dimers from a soft coral-derived *Alternaria* sp. fungus. *J. Nat. Prod.* **2012**, *75*, 189–197.
19. Parvatkar, R.R.; D'Souza, C.; Tripathi, A.; Naik, C.G. Aspernolides A and B, butenolides from a marine-derived fungus *Aspergillus terreus*. *Phytochemistry* **2009**, *70*, 128–132.
20. Li, H.J.; Lan, W.J.; Lam, C.K.; Yang, F.; Zhu, X.F. Hirsutane sesquiterpenoids from the marine-derived fungus *Chondrostereum* sp. *Chem. Biodivers.* **2011**, *8*, 317–324.
21. Zheng, C.J.; Shao, C.L.; Wu, L.Y.; Chen, M.; Wang, K.L.; Zhao, D.L.; Sun, X.P.; Chen, G.Y.; Wang, C.Y. Bioactive phenylalanine derivatives and cytochalasins from the soft coral-derived fungus, *Aspergillus elegans*. *Mar. Drugs* **2013**, *11*, 2054–2068.
22. Zhuang, Y.; Teng, X.; Wang, Y.; Liu, P.; Wang, H.; Li, J.; Li, G.; Zhu, W. Cyclopeptides and polyketides from coral-associated fungus, *Aspergillus versicolor* LCJ-5-4. *Tetrahedron* **2011**, *67*, 7085–7089.
23. Huang, X.S.; Huang, H.B.; Li, H.X.; Sun, X.F.; Huang, H.R.; Lu, Y.J.; Lin, Y.C.; Long, Y.H.; She, Z.G. Asperterpenoid A, a new sesterterpenoid as an inhibitor of *Mycobacterium tuberculosis* protein tyrosine phosphatase B from the culture of *Aspergillus* sp. 16-5c. *Org. Lett.* **2013**, *15*, 721–723.
24. Li, H.; Jiang, J.; Liu, Z.; Lin, S.; Xia, G.; Xia, X.; Ding, B.; He, L.; Lu, Y.; She, Z. Peniphenones A–D from the Mangrove Fungus *Penicillium dipodomyicola* HN4-3A as Inhibitors of *Mycobacterium tuberculosis* Phosphatase MptpB. *J. Nat. Prod.* **2014**, *77*, 800–806.
25. Xiao, Z.; Huang, H.; Shao, C.; Xia, X.; Ma, L.; Huang, X.; Lu, Y.; Lin, Y.; Long, Y.; She, Z. Asperterpenols A and B, new sesterterpenoids isolated from a mangrove endophytic fungus *Aspergillus* sp. 085242. *Org. Lett.* **2013**, *15*, 2522–2525.
26. Li, H.; Huang, H.; Shao, C.; Huang, H.; Jiang, J.; Zhu, X.; Liu, Y.; Liu, L.; Lu, Y.; Li, M.; *et al.* Cytotoxic norsesquiterpene peroxides from the endophytic fungus *Talaromyces flavus* isolated from the mangrove plant *Sonneratia apetala*. *J. Nat. Prod.* **2011**, *74*, 1230–1235.
27. Wen, L.; Cai, X.; Xu, F.; She, Z.; Chan, W.L.; Vrijmoed, L.L.P.; Jones, E.B.G.; Lin, Y. Three metabolites from the mangrove endophytic fungus *Sporothrix* sp. (#4335) from the South China Sea. *J. Org. Chem.* **2009**, *74*, 1093–1098.
28. Donatella, M.C.; Ronaldo, P.F.  $\alpha$ -Glucosidase inhibitors prevent diet-induced increases in intestinal sugar transport in diabetic mice. *Metabolism* **2006**, *55*, 832–841.
29. Mohan, S.; Eskandari, R.; Pinto, B.M. Naturally occurring sulfonium-ion glucosidase inhibitors and their derivatives: A promising class of potential antidiabetic agents. *Acc. Chem. Res.* **2014**, *47*, 211–225.
30. Calis, I.; Heilmann, J.; Tasdemir, D.; Linden, A.; Ireland, C.M.; Sticher, O. Flavonoid, iridoid, and lignan glycosides from *Putoria calabrica*. *J. Nat. Prod.* **2001**, *64*, 961–964.
31. Soman, A.G.; Gloer, J.B.; Wicklow, D.T. Antifungal and antibacterial metabolites from a sclerotium-colonizing isolate of *Mortierella vinacea*. *J. Nat. Prod.* **1999**, *62*, 386–388.
32. Yu, Z.; Smanski, M.J.; Peterson, R.M.; Marchillo, K.; Andes, D.; Rajski, S.R.; Shen, B. Engineering of *Streptomyces platensis* MA7339 for overproduction of platencin and congeners. *Org. Lett.* **2010**, *12*, 1744–1747.
33. Martin, J.A.; Vogel, E. The synthesis of zinniol. *Tetrahedron* **1980**, *36*, 791–794.

34. Rao, K.V.; Sadhukhan, A.K.; Veerender, M.; Ravikumar, V.; Mohan, E.V.; Dhanvantri, S.D.; Sitaramkumar, M.; Babu, J.M.; Vyas, K.; Reddy, G.O. Butyrolactones from *Aspergillus terreus*. *Chem. Pharm. Bull.* **2000**, *48*, 559–562.
35. Nuclear, P.; Sommit, D.; Boonyuen, N.; Pudhom, K. Butenolide and furandione from an endophytic *Aspergillus terreus*. *Chem. Pharm. Bull.* **2010**, *58*, 1221–1223.
36. Fуска, J.; Uhrín, D.; Proksa, B.; Votický, Z.; Ruppeltdt, J. The structure of vermistatin, a new metabolite from *Penicillium vermiculatum*. *J. Antibiot.* **1986**, *39*, 1605–1608.
37. Xia, X.; Huang, H.; She, Z.; Cai, J.; Liu, F.; Zhang, J.; Fu, L.; Vrijimoed, L.L.P.; Lin, Y.C. Structural and biological properties of vermistatin and two new vermistatin derivatives isolated from the marine-Mangrove endophytic fungus *Guignardia* sp. No. 4382. *Helv. Chim. Acta* **2007**, *90*, 1925–1931.
38. Brindis, F.; Rodríguez, R.; Bye, R.; González-Andrade, M.; Mata, R. (Z)-3-butylidenephthalide from *Ligusticum porteri*, an  $\alpha$ -glucosidase inhibitor. *J. Nat. Prod.* **2011**, *74*, 314–320.
39. Omar, R.; Li, L.; Yuan, T.; Seeram, N.P.  $\alpha$ -Glucosidase inhibitory hydrolyzable tannins from *Eugenia jambolana* seeds. *J. Nat. Prod.* **2012**, *75*, 1505–1509.
40. Suzuki, H.; Tahara, M.; Takahashi, M.; Matsumura, F.; Okabe, T.; Shimazu, A.; Hirata, A.; Yamaki, H.; Yamaguchi, H.; Tanaka, N.; *et al.* Resorthiomycin, a novel antitumor antibiotic. I. Taxonomy, isolation and biological activity. *J. Antibiot.* **1990**, *43*, 129–134.
41. Tahara, M.; Okabe, T.; Furihata, K.; Tanaka, N.; Yamaguchi, H.; Nishimura, T.; Suzuki, H. Revised structure of resorthiomycin. *J. Antibiot.* **1991**, *44*, 255.

© 2014 by the authors; licensee MDPI, Basel, Switzerland. This article is an open access article distributed under the terms and conditions of the Creative Commons Attribution license (<http://creativecommons.org/licenses/by/3.0/>).